Generation of intense ultrabroadband optical pulses by induced phase modulation in an argon-filled single-mode hollow waveguide

Naoki Karasawa and Ryuji Morita

Department of Applied Physics, Hokkaido University, and Core Research for Evolutional Science and Technology, Japan Science and Technology Corporation, Kita-13, Nishi-8, Kita-Ku, Sapporo 060-8628, Japan

Hidemi Shigekawa

Institute of Applied Physics, University of Tsukuba, and Core Research for Evolutional Science and Technology, Japan Science and Technology Corporation, 1-1-1 Tennodai, Tsukuba 305-8573, Japan

Mikio Yamashita

Department of Applied Physics, Hokkaido University, and Core Research for Evolutional Science and Technology, Japan Science and Technology Corporation, Kita-13, Nishi-8, Kita-Ku, Sapporo 060-8628, Japan

Received August 26, 1999

We experimentally demonstrate the generation of intense ultrabroadband optical pulses whose spectrum ranges from 300 to 1000 nm (700-THz bandwidth) with a well-behaved spectral phase and 23-μJ pulse energy by a novel, simple setup utilizing induced phase modulation (IPM) in an argon-filled single-mode hollow waveguide. Fundamental as well as second-harmonic pulses produced by one common femtosecond pulse from a Ti:sapphire laser-amplifier system are copropagated in the hollow waveguide. The effect of the delay time between the two input pulses on the IPM spectral broadening is clarified and confirmed to agree with the theoretical result. It is found that the compressed pulse duration from this pulse is 1.51 fs if its phase is completely compensated for.

OCIS codes: 060.4370, 060.7140, 320.5520, 320.5540, 320.7140.

Generation of an ultrabroadband optical pulse with a fluent frequency dependence of the phase is important for creating a monocyclelike optical pulse and for shaping multiwavelength optical pulses. Recently, generation of an ultrabroadband optical pulse by use of induced phase modulation[1] (IPM) as well as self-phase modulation (SPM) in a glass fiber was proposed,[2,3] and broadband pulse generation from 480 to 900 nm was experimentally demonstrated by use of a fundamental pulse and a signal pulse from an optical parametric amplifier based on a femtosecond Ti:sapphire laser system.[4]

Single-mode capillary fibers filled with noble gases have been used to broaden the spectrum of the optical pulses through dispersive SPM,[5,6] and sub-5-fs, high-powered pulses have been generated by use of this technique.[6] Also, 8-fs pulses at 400 nm have been generated with a similar approach.[7] Because of the chemical stability of noble gases, the damage threshold at the capillary fiber is relatively high[8] ($\sim$100 μJ) compared with that of a glass fiber. Also, the large walk-off length is advantageous for spectral broadening by use of IPM. We have analyzed nonlinear chirp from SPM and IPM in the case of two-pulse propagation in a single-mode capillary fiber and found that by choice of a proper delay time between pulses it is possible to generate ultrabroadband pulses whose spectrum covers the near infrared to the near ultraviolet, with a fluent frequency dependence of the phase by means of a practical setup.[9] Since the second-harmonic and the fundamental waves are generated from one common femtosecond pulse, the carrier-phase difference between their waves is constant.[10,11] This enables us to synthesize constructively two spectrally broadened waves at the fiber output. In this Letter an experimental verification of this analysis is presented.

The experimental setup is shown in Fig. 1. The output beam of a Ti:sapphire laser-amplifier system (Femtopower 1000; center wavelength, $\sim$790 nm; pulse width, 24 fs; repetition rate, 1 kHz; pulse energy, 1 mJ) is passed through a 0.5-mm-thick β-barium borate (BBO) crystal (C_1). Second-harmonic pulses generated by type I phase matching are separated from fundamental pulses by two harmonic separators (HS's). We rotate the polarization direction of the fundamental pulses by 90° by use of two periscopes (PS) to match it with that of the second-harmonic pulses. The

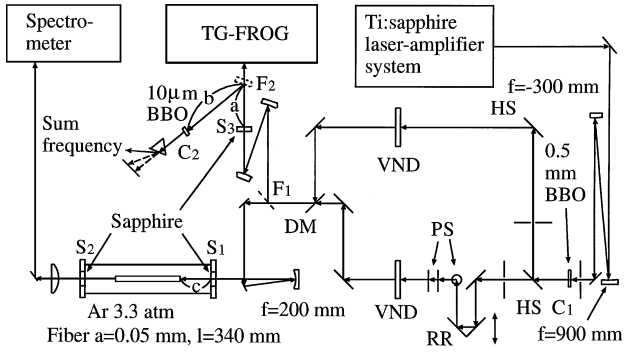

Fig. 1. Experimental setup of ultrabroadband optical pulse generation. See text for definitions.

0146-9592/00/030183-03$15.00/0

fundamental and the second-harmonic pulses are combined by use of dichroic mirror (DM) and collimated by a spherical mirror with a 20-cm focal length. A capillary fiber with a 34-cm length and a 0.1-mm inner diameter is positioned in a chamber filled with argon gas with a pressure of 3.3 atm. The chamber has two 1-mm-thick sapphire windows (S_1 and S_2). A retroreflector (RR) is used to adjust the delay time of the second-harmonic pulses with respect to the fundamental pulses. The input energies of the pulses are adjusted by use of variable neutral-density filters (VND's). Both input pulses are redirected by a flip mirror (F_1) and evaluated by use of a transient-grating frequency-resolved optical gating (TG-FROG) apparatus.[12] To include the influence of the sapphire window, S_1, we adjust the beam sizes and pass the beams through the equivalent sapphire plate, S_3, before they enter the TG-FROG apparatus. The measured time-dependent intensities and phases are used for numerical calculations. To calibrate the delay time between the fundamental and the second-harmonic pulses, we use a 10-μm-thick BBO crystal (C_2) to generate sum-frequency pulses from these pulses. To avoid the necessity of positioning the crystal inside the chamber we redirect the pulse beams by use of a flip mirror, F_2, and focus them at the crystal. The crystal is positioned such that the product of the path length and $d = 1/v_{g2} - 1/v_{g1}$, and v_{gi}, the group velocity of the pulse i (the subscripts 1 and 2 represent the fundamental and the second-harmonic, respectively), is equivalent to the original path to the fiber entrance, i.e., $(a + b) \times d_{\text{air}} = c \times d_{\text{Ar, 3.3atm}}$ in Fig. 1. Also, S_3 is positioned so that the path length from F_1 to S_1 is equal to that from F_1 to S_3. The delay position that gives the largest sum-frequency signal is determined as the delay time 0 ($T_d = 0$), which corresponds to the situation in which both the fundamental and the second-harmonic pulses coincide at the fiber input end. A negative T_d corresponds to the case in which the second-harmonic pulse enters the fiber before the fundamental pulse.

Fundamental pulses of 40.8-μJ energy and second-harmonic pulses of 37.8-μJ energy are focused at the fiber entrance. Figures 2(a)–2(c) show the spectra at the output of a fiber. In Fig. 2(a), two spectra obtained when the two pulses are propagated separately are shown. In this case the spectral broadening is due to only SPM. When the delay time between two copropagated pulses is adjusted so that these pulses overlap inside the fiber, we observe larger spectral broadening owing to IPM and SPM [Figs. 2(b) and 2(c)]. Inside the fiber, $d = 185$ fs/m, and thus the propagation-time difference between the fundamental and the second-harmonic pulses for the entire fiber length of 34 cm is 63 fs (185 fs/m $\times$ 0.34 m). Figure 2(b) shows the spectrum obtained when the two pulses meet near the fiber entrance ($T_d = 13$ fs). It can be observed that the spectral intensity near both edges [the spectral intensity at shorter wavelengths than the second harmonic (less than ~400 nm) and longer wavelengths than the fundamental (more than ~800 nm)] increases, but it does not increase much at the middle. Figure 2(c) shows the spectrum when the two pulses meet near the fiber exit ($T_d = -80$ fs). In this case, unlike in Fig. 2(b), an intensity increase of the spectrum can be observed in the middle section (450–550 nm); in particular, a new peak can be observed near 480 nm. The best overlap of the spectrum between two pulses, with more-homogeneous broadening from 300 to 1000 nm (700-THz bandwidth), is observed at this delay time. This delay-time dependence of the spectral broadening agrees well with our previous theoretical prediction.[9] Also, the peak powers that are required for spectrum overlap of the two pulses are consistent with those of our theoretical analysis.[9]

The total output pulse energy is 23.0 μJ (29.3% efficiency), corresponding to 11.9 and 11.1 μJ for the fundamental and the second-harmonic pulses, respectively. These corresponding output energies give energy throughput of 29.2% (11.9/40.8) for the fundamental and 29.4% (11.1/37.8) for the second-harmonic pulse. However, the coupling loss at the fiber input is unknown. To determine this quantity we perform numerical calculations to obtain the spectral broadening at various input-pulse energies for SPM (Ref. 9) and compare them with spectra obtained from SPM experiments. In the calculations the temporal intensity and the phase profile as measured by TG-FROG for the fundamental and the second-harmonic pulses are used. The calculations include accurate dispersion effects resulting from the argon gas[13] and the waveguide mode[14] and a SPM nonlinear term with self-steepening. In the calculations the following parameters are used: $\lambda_c = 767.95$ nm, $T_p = 24$ fs, $P_0 = 1.03$ GW (values of $P_0 = 0.12, 0.29$, and 0.57 GW are also used, but the calculations are not shown directly here), and $n_2 = 2.99 \times 10^{-23}$ m^2/W for

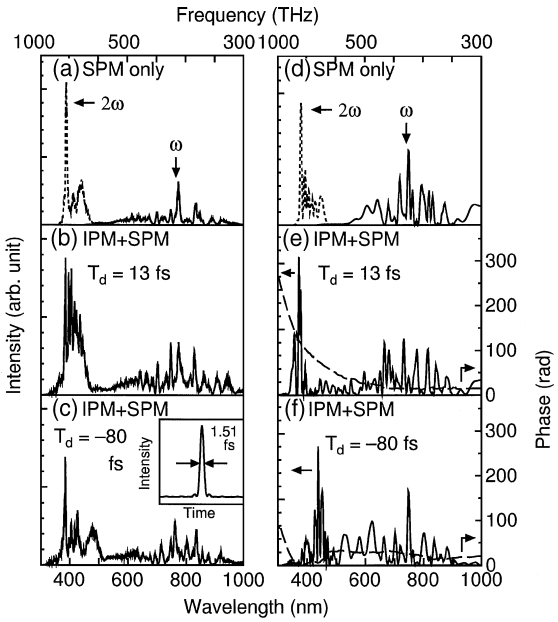

Fig. 2. (a)–(c) Experimental and (d)–(f) calculated spectra when the fundamental and the second-harmonic pulses are propagated separately and are copropagated in a fiber: (a), (d) SPM only; (b), (e) IPM + SPM, $T_d = 13$ fs; (c), (f) IPM + SPM, $T_d = -80$ fs. In the inset in (c), the temporal intensity of the inverse Fourier transform of the spectrum, assuming a constant phase, is shown.

fundamental pulses, and $\lambda_c = 404.84$ nm, $T_p = 58$ fs, $P_0 = 0.46$ GW (0.073, 0.20 GW are also used but not shown), and $n_2 = 4.78 \times 10^{-23}$ m^2/W for second-harmonic pulses, where λ_c is the center wavelength, T_p is the pulse width, P_0 is the peak power, and n_2 is the nonlinear refractive index.[15] The effective core area[16] of the EH_{11} mode is calculated to be $0.477\pi a^2$, where a is the radius of the capillary fiber. Here we assume that the spatial profile of the electric field for its mode is $J_0(2.405r/a)$,[14] where J_0 is the zeroth-order Bessel function. The nonlinear refractive index is taken from Ref. 17, and we use different values of n_2 for the fundamental and the second-harmonic waves, taking into account the dispersion of this n_2 parameter. The theoretical propagation loss that is due to the waveguide itself[14] is 52% for the fundamental wave and 17% for the second-harmonic wave. If we consider only this loss, the net input energy evaluated from the output energy (11.9 μJ) for the fundamental wave is 24.8 μJ (11.9 μJ/0.48). The calculated spectral broadening obtained by use of SPM with this value (24.8 μJ) agrees with the experimental broadening. We have also verified this agreement, using different input-pulse energies. Thus the coupling loss at the fiber entrance (in microjoules) is evaluated to be 39% [(40.8 − 24.8)/40.8]. For the second-harmonic wave, the net input energy evaluated from output energy by consideration of the theoretical waveguide loss is 13.4 μJ (11.1 μJ/0.83). However, it was necessary that we set 26.7 μJ as the practical input-pulse energy to obtain similar broadening in SPM experiments. Therefore, the coupling loss (in microjoules) becomes 29% [(37.8 − 26.7)/37.8] for this case. This coupling loss has also been confirmed for different input-pulse energies. The reason for this difference is probably defects such as microbending, whose effect becomes remarkable for shorter wavelengths, inside the fiber.[14] In Figs. 2(d)–2(f), the numerically calculated spectra obtained with the parameters thus determined are shown. In Fig. 2(d), the calculated spectra for SPM for the fundamental and the second-harmonic waves are shown. In Figs. 2(e) and 2(f), the calculated spectra for IPM + SPM at two different delay times are shown. It can be seen that the relative spectral intensity around the central part from 400 to 800 nm is larger in Fig. 2(f) than in Fig. 2(e). In addition, the more-homogeneous spectrum broadens from 300 to 1000 nm in Fig. 2(f) compared with that in Fig. 2(e). These behaviors agree with those shown by the experimental spectra. In Figs. 2(e) and 2(f), the calculated wavelength-dependent phases are shown. It can be seen that the phase variations are relatively smooth, which is important for phase compensation for pulse compression and synchronous multicolor shaping.

In the inset of Fig. 2(c), the inverse Fourier transform of the experimental spectrum of Fig. 2(c) when its spectral phase is set to be constant is shown. The evaluated pulse duration is 1.51 fs. Since this spectrum is generated by the interaction between two pulses, the chirp is not expected to be linear, and thus it is necessary to use a method that can compensate for the nonlinear chirp. One such method is the use of an adaptive spatial light modulator, which has the potential for generating a monocyclelike pulse.

In conclusion, ultrabroadband (300–1000 nm) optical pulse generation by use of IPM as well as SPM in a gas-filled single-mode hollow waveguide has been experimentally demonstrated. By utilizing fundamental as well as second-harmonic pulses from a femtosecond Ti:sapphire laser-amplifier system in an argon-filled capillary fiber, we observed pulses whose spectrum covers the near infrared (1000 nm) to the near ultraviolet (300 nm). To our knowledge this is the broadest coherent spectrum (700-THz bandwidth) with a well-behaved spectral phase that has been obtained. The coupling loss was evaluated by comparison of the SPM experimental and calculated spectra. The IMP + SPM spectral broadening behavior as a function of the delay time has been experimentally clarified, and agreement with the theoretical analysis has been confirmed.

References

1. P. L. Baldeck, P. P. Ho, and R. R. Alfano, in *The Supercontinuum Laser Source*, R. R. Alfano, ed. (Springer-Verlag, Berlin, 1989), p. 117.
2. M. Yamashita, H. Sone, and R. Morita, Jpn. J. Appl. Phys. **35,** L1194 (1996).
3. M. Yamashita, H. Sone, R. Morita, and H. Shigekawa, IEEE J. Quantum Electron. **34,** 2145 (1998).
4. L. Xu, N. Karasawa, N. Nakagawa, R. Morita, H. Shigekawa, and M. Yamashita, Opt. Commun. **162,** 256 (1999).
5. M. Nisoli, S. De Silvestri, and O. Svelto, Appl. Phys. Lett. **68,** 2793 (1996).
6. M. Nisoli, S. Stagira, S. De Silvestri, O. Svelto, S. Sartania, Z. Cheng, M. Lenzner, Ch. Spielmann, and F. Krausz, Appl. Phys. B **65,** 189 (1997).
7. O. Dühr, E. T. J. Nibbering, G. Korn, G. Tempea, and F. Krausz, Opt. Lett. **24,** 34 (1999).
8. G. Tempea and T. Brabec, Opt. Lett. **23,** 762 (1998).
9. N. Karasawa, R. Morita, L. Xu, H. Shigekawa, and M. Yamashita, J. Opt. Soc. Am. B **16,** 662 (1999).
10. E. Sidick, A. Knoesen, and A. Dienes, J. Opt. Soc. Am. B **12,** 1704 (1995); E. Sidick, A. Dienes, and A. Knoesen, J. Opt. Soc. Am. B **12,** 1713 (1995).
11. R. Wynands, O. Coste, C. Rembe, and D. Meschede, Opt. Lett. **20,** 1095 (1995).
12. J. N. Sweetser, D. N. Fittinghoff, and R. Trebino, Opt. Lett. **22,** 519 (1997).
13. A. Dalgarno and A. E. Kingston, Proc. R. Soc. London Ser. A **259,** 424 (1960).
14. E. A. J. Marcatili and R. A. Schmeltzer, Bell Syst. Tech. J. **43,** 1783 (1964).
15. We adjusted the angle of BBO crystal to obtain the best spectral broadening owing to IPM and SPM at the fiber output. In this situation the spectrum of the fundamental pulse at the fiber input is modulated, and the center wavelength of the fundamental pulse is not equal to that of the second-harmonic pulse.
16. G. P. Agrawal, *Nonlinear Fiber Optics* (Academic, San Diego, Calif., 1989).
17. H. J. Lehmeier, W. Leupacher, and A. Penzkofer, Opt. Commun. **56,** 67 (1985).